Quaternary Research 76 (2011) 272–284

Contents lists available at ScienceDirect

Quaternary Research

journal homepage: www.elsevier.com/locate/yqres

QR Forum

Chronology of latest Pleistocene mountain glaciation in the western Wasatch Mountains, Utah, U.S.A.

Benjamin J.C. Laabs [a,*], David W. Marchetti [b], Jeffrey S. Munroe [c], Kurt A. Refsnider [d], John C. Gosse [e], Elliott W. Lips [f], Richard A. Becker [g], David M. Mickelson [g], Brad S. Singer [g]

[a] Department of Geological Sciences, SUNY Geneseo, 1 College Circle, Geneseo, New York, USA, 14454
[b] Geology Program, Western State College of Colorado, USA
[c] Department of Geology, Middlebury College, Vermont, USA
[d] INSTAAR, University of Colorado-Boulder, USA
[e] Department of Earth Sciences, Dalhousie University, Nova Scotia, Canada
[f] Department of Geography, University of Utah, USA
[g] University of Wisconsin-Madison, USA

ARTICLE INFO

Article history:
Received 23 November 2010
Available online 2 August 2011

Keywords:
Mountain glaciation
Great Basin
Wasatch Mountains
Lake Bonneville
Cosmogenic exposure dating

ABSTRACT

Understanding the timing of mountain glacier and paleolake expansion and retraction in the Great Basin region of the western United States has important implications for regional-scale climate change during the last Pleistocene glaciation. The relative timing of mountain glacier maxima and the well-studied Lake Bonneville highstand has been unclear, however, owing to poor chronological limits on glacial deposits. Here, this problem is addressed by applying terrestrial cosmogenic ^{10}Be exposure dating to a classic set of terminal moraines in Little Cottonwood and American Fork Canyons in the western Wasatch Mountains. The exposure ages indicate that the main phase of deglaciation began at 15.7 ± 1.3 ka in both canyons. This update to the glacial chronology of the western Wasatch Mountains can be reconciled with previous stratigraphic observations of glacial and paleolake deposits in this area, and indicates that the start of deglaciation occurred during or at the end of the Lake Bonneville hydrologic maximum. The glacial chronology reported here is consistent with the growing body of data suggesting that mountain glaciers in the western U.S. began retreating as many as 4 ka after the start of northern hemisphere deglaciation (at ca. 19 ka).

Introduction

In most settings in the western United States, resolving age relationships between Pleistocene glacial and lacustrine deposits is complicated by unclear stratigraphic relationships and few numerical age limits on glacial deposits. For example, radiocarbon chronologies suggest that the two largest Great Basin paleolakes – Lahontan and Bonneville – reached their maximum areal extents *after* the end of the global Last Glacial Maximum (LGM; ~19 ka; Clark et al., 2009). Lake Bonneville reached its maximum extent at 18.7 to 17.6 cal ka BP (Oviatt, 1997) and Lake Lahontan at ca. 16 cal ka BP (Benson et al., 1990; Adams and Wesnousky, 1998; all ^{14}C ages discussed herein are calibrated using CALIB 6.0; Reimer et al., 2009). In contrast, a smaller number of radiocarbon ages of glacial deposits (or glacially derived sediment deposited in lakes) limit the timing of mountain glacier maxima in the western U.S. to the global LGM (e.g., Madsen and Currey, 1979) or *earlier* (e.g., Rosenbaum and Heil, 2009), leading to the view that Great Basin paleolakes attained their maximum areal extent while mountain glaciers were retreating (e.g., Scott et al., 1983; Benson and Thompson, 1987). Finally, terrestrial cosmogenic nuclide (TCN) surface-exposure ages of some Pleistocene terminal moraines near the eastern border of the Great Basin region suggest that glacier and paleolake maxima were nearly synchronous (e.g., Licciardi and Pierce, 2008; Briner, 2009; Laabs et al., 2009).

The relative timing of paleolake and mountain glacier changes in the Great Basin has important implications for understanding how climate changed in the western U.S. during the last glaciation and subsequent deglaciation. The relative importance of temperature and precipitation controls on lake and glacier mass balance in this region has long been a topic of controversy. Some studies suggest a cold and dry climate in the interior western U.S. during MIS 2 (marine oxygen isotope stage 2; e.g., Galloway, 1970; Porter et al., 1983; Kaufman, 2003) while others suggest that greater-than-modern precipitation drove expansion of paleolakes and glaciers (e.g., Benson and Thompson, 1987). Firmly establishing the relative timing of paleolake and mountain glacier changes would provide an important framework for regional circulation

* Corresponding author.
E-mail addresses: laabs@geneseo.edu (B.J.C. Laabs), dmarchetti@western.edu (D.W. Marchetti), jmunroe@middlebury.edu (J.S. Munroe), Kurt.Refsnider@Colorado.Edu (K.A. Refsnider), john.gosse@dal.ca (J.C. Gosse), elips@geog.utah.edu (E.W. Lips), rabecker@geology.wisc.edu (R.A. Becker), davem@geology.wisc.edu (D.M. Mickelson), bsinger@geology.wisc.edu (B.S. Singer).

0033-5894/$ – see front matter © 2011 University of Washington. Published by Elsevier Inc. All rights reserved.
doi:10.1016/j.yqres.2011.06.016

model experiments that could resolve this issue, and could help to improve the understanding of mountain glacier sensitivity to climate change (e.g., Thackray, 2008).

This study capitalizes on a rare setting in which stratigraphic relationships between glacial and lacustrine deposits are observed and where a classic set of Pleistocene terminal moraines provides abundant material suitable for terrestrial cosmogenic nuclide (TCN) surface-exposure dating at the western front of the Wasatch Mountains. Here, shoreline deposits of Lake Bonneville are well preserved in a widely known locale where Pleistocene moraines clearly limit the extent of glaciers (Richmond, 1964; Scott and Shroba, 1985; Personius and Scott, 1992). Through application of TCN ^{10}Be surface-exposure dating, age limits on the start of deglaciation from a set of terminal moraines in Little Cottonwood and American Fork canyons (Fig. 1) are significantly improved and compared to an established radiocarbon-based hydrograph of Lake Bonneville (Oviatt, 1997; Godsey et al., 2005a). The paleoclimatic implications of the new age limits on the timing of the last glaciation in the Wasatch Mountains and paleolake maxima are discussed, along with the temporal offset between the start of northern hemisphere deglaciation (at 20 to 19 ka) and regional deglaciation in the western U.S.

Previous studies in the western Wasatch Mountains

Glacial and paleolake deposits at the front of the western Wasatch Mountains have been studied for over a century, with early reports including some morpho-stratigraphic relationships of glacial and paleolake features (Gilbert, 1890; Richmond, 1964; Morrison, 1965) and later reports presenting stratigraphic observations within the vicinity of the Wasatch Fault Zone (Scott and Shroba, 1985; Personius and Scott, 1992). These studies provide an intriguing historical progression of ideas of whether glaciers in the western Wasatch Mountains or Lake Bonneville attained their respective maxima first (Scott, 1988), and further illustrate the need for direct chronological constraints on glacial deposits in the western Wasatch Mountains. Although the early report of Gilbert (1890) does not describe stratigraphic observations between lacustrine and glacial deposits, he proposes that the timing of glacier and lake expansion was nearly synchronous. Later reports by Richmond (1964) and Morrison (1965) place deposits of Lake Bonneville and mountain glaciers in Little Cottonwood and Bells Canyons into the context of the Rocky Mountain model of Pleistocene glaciations, based largely on weathering characteristics of tills and stratigraphic observations. Following the availability of radiocarbon ages on shoreline deposits of Lake Bonneville (Broecker and Kaufman, 1965) and on tills in Little Cottonwood Canyon (Madsen and Currey, 1979), Scott and Shroba (1985) revise Richmond's glacial mapping to show that the mouths of both canyons were occupied by glacier ice during the Pinedale Glaciation (the last Pleistocene glaciation in the Rocky Mountains) (Fig. 1). Furthermore, they report shoreline gravels of Lake Bonneville stratigraphically overlying Pinedale-equivalent tills comprising the distal slope of the terminal moraine at Bells Canyon (immediately south of Little Cottonwood Canyon). Finally, Scott et al. (1983) note a 0.5-m-thick, weakly developed soil in till overlain by shoreline gravel, and interpret this to indicate that ice retreat began in Little Cottonwood Canyon at least 3000 yr before the Lake Bonneville highstand. This evidence, combined with several other locales where Richmond (1964) describes Lake Bonneville deposits stratigraphically above (undated) tills, indicates ice presence at the canyon mouths at some interval prior to the Lake Bonneville highstand. However, based on the relatively broad age limits on tills underlying Lake Bonneville shoreline gravels at Little Cottonwood Canyon, it cannot be discerned whether ice occupied the mouth of the canyon prior to the Lake Bonneville highstand during MIS 2 or an earlier glacial interval (e.g., MIS 4, 5d, or 6).

Some recent observations suggest that glaciers occupied the mouth of Little Cottonwood and Bells Canyons after the Bonneville highstand. Godsey et al. (2005b) document till overlying and underlying shoreline gravels of Lake Bonneville exposed in trenches excavated at the toe of the right-lateral sector of the terminal moraine at Little Cottonwood Canyon (Fig. 1). They interpret this stratigraphy, which is consistent with the most recent surficial geologic mapping (Personius and Scott, 1992), to represent two ice advances to the mouth of the canyon during MIS 2, one before and one after the Lake Bonneville highstand.

Chronology of Lake Bonneville

The current chronological limits on shoreline elevations of the lake are summarized here to provide chronological reference for the discussion of cosmogenic ^{10}Be exposure ages of terminal moraines. Throughout the Pleistocene, paleolakes in the Bonneville basin fluctuated to surface elevations of as much as ~300 m above the modern average elevation of Great Salt Lake. The most recent expansion started prior to the end of the global LGM when the lake began rising to form Lake Bonneville, which reached a maximum elevation of ~1550 m asl at ~18.7 cal ka BP (based on an age of 15.5 ^{14}C ka BP for the Pavant Butte ash; Oviatt and Nash, 1989; Oviatt, 1997). Lake Bonneville persisted at this level until ~17.6 cal ka BP (based on an age of 14.5 ^{14}C ka BP for the Bonneville Flood lithologic marker, Oviatt et al., 1994; Oviatt, 1997). Lake Bonneville subsequently fell ~100 m to the Provo shoreline (~1450 m asl) due to failure of a topographic threshold at the northern end of the basin (Gilbert, 1890; O'Connor, 1993). The lake level oscillated near this elevation and continued overflowing until about 15.0 cal ka BP (Godsey et al., 2005a) before dropping rapidly to elevations near that of the modern Great Salt Lake (~1280 m asl).

Glacial geology and terminal moraines in Little Cottonwood and American Fork Canyons

Terminal moraines at the mouth of Little Cottonwood Canyon and within American Fork Canyon (Fig. 1) were targeted for TCN ^{10}Be exposure dating. Large quartz monzonite boulders are common atop two sectors of the terminal moraine at Little Cottonwood Canyon (Fig. 1). The first area sampled for this study is a tall, sharp-crested left-lateral moraine on the south side of the canyon that is vertically offset in multiple places by the Wasatch Fault and ends abruptly at the western front of the Wasatch Mountains (Fig. 1). The second sampled area comprises low-relief ridges of the right-lateral sector of the terminal moraine on the north side of the canyon mouth (Fig. 1). The distal slope of this sector is above 1550 m asl, close to the shoreline elevation of the Lake Bonneville highstand. Although this sector forms the outermost moraine ridge on the north side of Little Cottonwood Canyon, it does not delimit the outermost extent of Pinedale-equivalent tills (Scott and Shroba, 1985; Personius and Scott, 1992). Till layers extend beyond the terminal moraine on the north side of the canyon to elevations below 1550 m asl and in places are buried by shoreline gravels of Lake Bonneville (Richmond, 1964; Morrison, 1965; Scott and Shroba, 1985). Scott et al. (1983) describe shoreline gravels stratigraphically above weakly weathered till (which they mapped as Pinedale-equivalent based on its weathering characteristics) approximately 200 m beyond the right-lateral sector of the terminal moraine (Fig. 1); the outermost extent of this till is unknown.

The terminal moraine in American Fork Canyon exhibits two ridge crests, both displaying some low-relief hummocky topography. In this canyon, ice did not extend to the canyon mouth and the moraine is situated high above the maximum shoreline elevation of Lake Bonneville. Quartzite boulders (derived from the Tintic and Big Cottonwood Formations; Bryant, 1992), many displaying glacial polish, are abundant atop both ridges of this moraine. Boulders atop

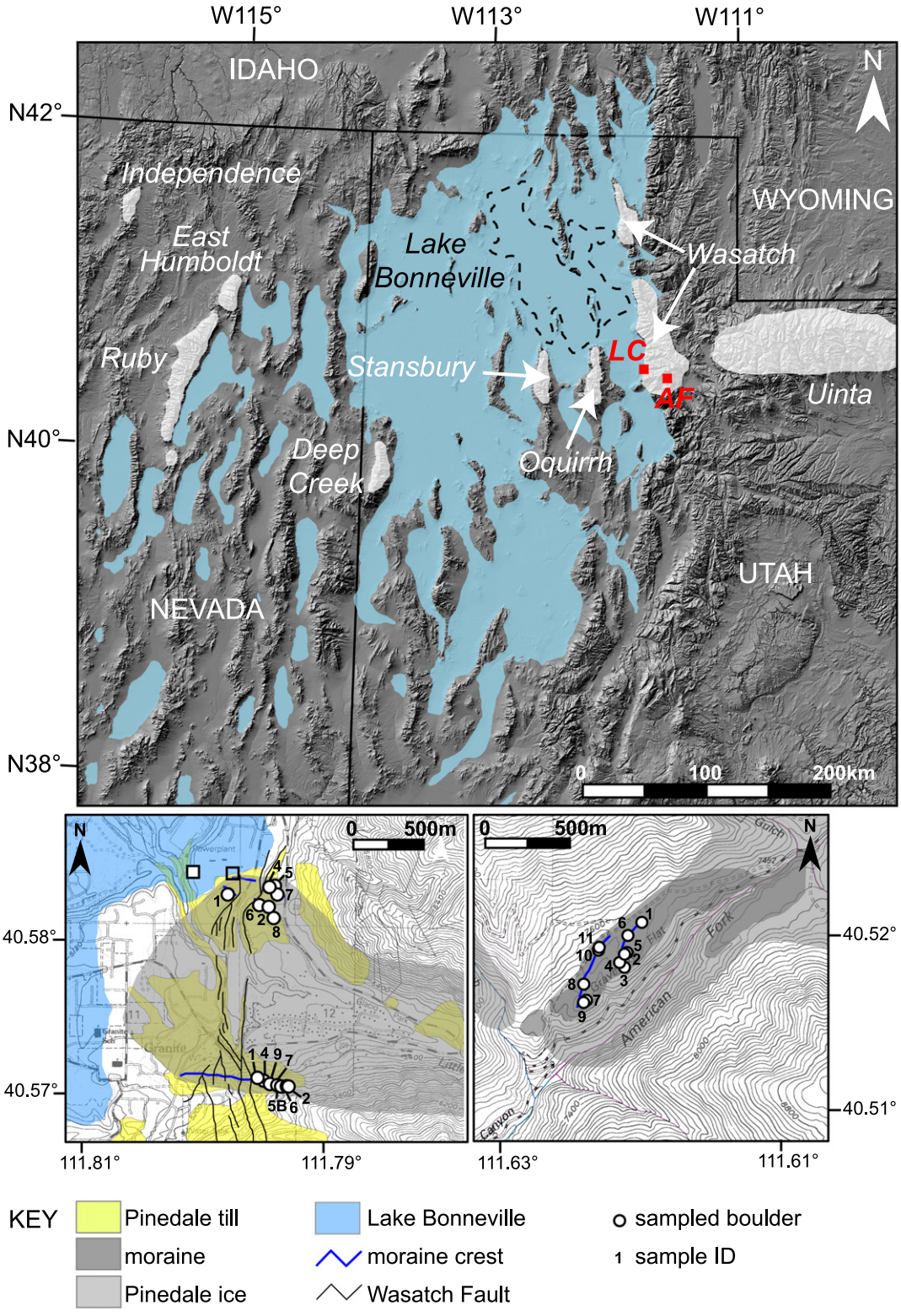

Figure 1. Top panel: Shaded-relief map of a portion of the interior western United States (elevation data are from the National Elevation Dataset; http://www.ned.usgs.gov). Blue areas indicate the extent of Lake Bonneville and other Great Basin lakes. White areas are select mountain ranges (or portions thereof) that contained valley glaciers during the latest Pleistocene. Dashed line indicates the approximate extent of Great Salt Lake. Red boxes are the locations of the two study areas, Little Cottonwood (LC) and American Fork (AF) Canyons. Lower panels: topographic maps displaying glacial geology and TCN ^{10}Be sample locations at (left) Little Cottonwood Canyon and (right) American Fork Canyon. The extent of Pinedale-equivalent till at Little Cottonwood Canyon (yellow) and the approximate extent of Lake Bonneville (light blue) are based on surficial geologic mapping of Scott and Shroba (1985). Numbered sample locations correspond to the last digit of the sample IDs given in Tables 1 and 2. White box indicates the site where Scott et al. (1983) describe shoreline gravels of Lake Bonneville stratigraphically above weakly weathered Pinedale-equivalent till. White box indicates the site where Godsey et al. (2005a) describe Pinedale-equivalent till stratigraphically above and below shoreline gravels of Lake Bonneville. Topographic maps are from the U.S. Geological Survey 7.5 minute series, displaying portions of the Draper (left) and Bridal Veil Falls (right) quadrangles.

both ridge crests were sampled to evaluate whether they represent significantly different intervals of glacier maxima (Fig. 1).

TCN ^{10}Be surface exposure dating methods

The largest erratic boulders atop the moraines described above were sampled for TCN ^{10}Be exposure dating (sample sites are shown in Fig. 1). Samples were collected with a hammer and chisel, chemically-prepared following methods of Gosse and Phillips (2001) and Munroe et al. (2006) (the latter derived from Bierman et al., 2002), and analyzed for concentrations of TCN ^{10}Be in quartz by accelerator mass spectrometry (AMS; Muzikar et al., 2003). TCN exposure ages were calculated with the CRONUS-Earth online calculator (Balco et al., 2008; Version 2.2; http://hess.ess.washington.edu/math/) and are based on a temporally-constant spallogenic and muonic production rate of ^{10}Be in quartz. Spallogenic production is scaled for latitude and geographic altitude from Lal (1991) and Stone (2000) for all sampled boulders. For coarse-grained quartz monzonite boulders, production is also scaled for a boulder-surface erosion rate of 0.0003 cm/yr inferred from physical weathering characteristics.

Results and interpretation— chronology of glaciation in the western Wasatch Mountains

At Little Cottonwood Canyon, the set of exposure ages from atop the right-lateral moraine is less variable (coefficient of variation, CV = 4.4%) than that determined for the left-lateral moraine (CV = 31%; Tables 1 and 2). Although variability of ~30% is not uncommon for TCN exposure ages of moraine boulders (Putkonen and Swanson, 2003), the contrasting variability between the two sectors of the moraine warrants further discussion.

Variability among exposure ages from the left-lateral moraine may reflect (i) repeated occupation of the moraine during the latest Pleistocene, (ii) variable erosion of boulder surfaces, (iii) boulder overturning due to seismic shaking, (iv) boulder exhumation, (v) inheritance of ^{10}Be from exposure prior to final deposition on the moraine crest, or (vi) differences in geochemical preparation or AMS analysis. The effects of boulder erosion or overturning should affect the two sampled sectors of the terminal moraine equally (given the proximity of the sectors to one another and to the Wasatch Fault; Fig. 1), and can therefore be ruled unlikely. Differences in geochemical preparation methods of all the samples from the two sectors provide no compelling explanation of the observed variability. The potential impacts of inherited ^{10}Be and/or boulder exhumation are possible, and distinguishable in theory. For example, although the two oldest ^{10}Be exposure ages from this moraine are consistent with radiocarbon age limits on till at the mouth of the Little Cottonwood Canyon (Madsen and Currey, 1979), it is also possible that these boulders contain inherited ^{10}Be from prior exposure on the steep wall near the mouth of the canyon. The variability of exposure ages could also be suggestive of boulder exhumation due to degradation of the moraine crest (e.g., Putkonen and Swanson, 2003). Field measurements indicate that the left-lateral moraine is taller (~60 m vs. 20 m of relief) and steeper (~20% vs. ~3% gradients) than the right-lateral moraine and, therefore, may have experienced a greater degree of crest lowering, which could be reflected by the two youngest exposure ages. Unfortunately, the distribution of ^{10}Be exposure ages from this moraine is not consistent with either inherited ^{10}Be or boulder exhumation (Applegate et al., 2010), and the relative contributions of these factors to the variability of ^{10}Be exposure ages from the left-lateral sector of the moraine remain unclear. However, as noted by Douglass et al. (2006), the mean square of weighted deviates (MSWD) statistic of a set of ^{10}Be exposure ages from a single moraine can indicate whether the observed variability of a set of ages is consistent with the expected variability as defined by the error of the AMS measurement. A large MSWD value (greater than 1) indicates that either measurement errors are underestimated, or that systematic errors caused by geological processes have resulted in a broad scatter of exposure ages.

Based on the great differences in MSWD values (2.5 and 6.8 for the American Fork and right-lateral sector of the Little Cottonwood moraine, respectively; 38 for the left-lateral sector of the Little Cottonwood moraine) for the sets of ^{10}Be exposure ages from the three moraine sectors sampled in the western Wasatch Mountains (Table 1), we conclude that geologic processes have affected the distribution of ages on the left lateral sector of the terminal moraine at Little Cottonwood Canyon to a greater extent compared to the right-lateral sector of the terminal moraine and the American Fork terminal moraine. Therefore, the chronological limits on the start of deglaciation in the western Wasatch Mountains described below are based only on ^{10}Be exposure ages from the right-lateral sector of the terminal moraine at Little Cottonwood Canyon and the terminal moraine at American Fork Canyon.

The mean ^{10}Be exposure age ($\pm 1\sigma$) from the right-lateral sector of the terminal moraine at Little Cottonwood Canyon is interpreted to indicate that this sector was abandoned by glacier ice at 15.7 ± 0.7 ka ($n = 7$; Fig. 2). The mean ^{10}Be exposure age of 16.4 ± 5.0 ka ($n = 7$) from the left-lateral sector is statistically similar, but with a greater standard deviation for reasons described above. Exposure ages from the American Fork Canyon moraine yield a mean age of 15.7 ± 1.6 ka ($n = 10$), which is also interpreted to indicate the time when that moraine was abandoned by ice (Fig. 2). These ages suggest that glaciers occupied terminal moraines in the western Wasatch Mountains until approximately 15.7 ± 1.3 ka, the mean of all ^{10}Be exposure ages from the right-lateral sector of the Little Cottonwood moraine and from the American Fork moraine ($\pm 1\sigma$). Although the 1σ range of the distribution of ages on these two moraines does not incorporate the measurement error of each individual exposure age, it is similar to the 95% confidence interval associated with the error-weighted mean calculation. The 1σ range also avoids weighting the younger ^{10}Be exposure ages (with lesser 1σ errors) greater than older ^{10}Be exposure ages (with greater 1σ errors), which may not be appropriate (Applegate et al., 2010).

The results of this study indicate that ice retreat began in the western Wasatch Mountains while Lake Bonneville was overflowing at the Provo level. Although some previous studies interpret the record at Little Cottonwood Canyon to indicate that ice retreat began prior to the Lake Bonneville highstand (Madsen and Currey, 1979; Scott et al., 1983), there are several reasons why uncertainty in the TCN ^{10}Be production rates fails to explain the younger exposure ages reported here. First, the four time-dependent production-rate scaling methods recommended by the CRONUS-Earth project (Balco et al., 2008), which treat the effect of geomagnetic field variations on production rate differently, yield exposure ages that are all within 0.5 ka of those determined by a constant production rate model (Table 2). The exposure ages computed from time-dependent scaling models do have a greater 1σ error estimate (9 to 13% compared to 2 to 8% for the constant production rate model), reflecting the combined error of the scaled production rate and the AMS measurement. However, even when an error of 13% is applied to the mean of the ages from each moraine determined from the time-dependent models (16.0 ± 2.1 ka for the right lateral moraine at Little Cottonwood Canyon; 15.3 ± 2.0 ka for the American Fork moraine), the mean of these exposure ages (15.8 ± 1.2 ka, 1σ) still suggests that ice retreat began during or after the Lake Bonneville highstand (18.7 to 17.6 cal ka BP). Second, the distribution of ^{10}Be exposure ages from the northern sector of the terminal moraine at Little Cottonwood Canyon and from the American Fork moraine does not exhibit the broad variability of exposure ages typical of degraded moraines (Applegate et al., 2010), suggesting that geomorphic processes have not significantly contributed to error of exposure ages. Third, deglaciation commencing at 15.7 ± 1.3 ka is consistent with a limiting radiocarbon age on till up valley of the Little Cottonwood Canyon

Table 1
^{10}Be Data and TCN exposure ages for terminal moraines in the western Wasatch Mountains.

Sample locale	Sample Id	Elevation (m asl)	Latitude (°N)	Longitude (°W)	[^{10}Be] (atoms·g SiO_2^{-1})[a]	1σ	Boulder height (m)	Sample thickness (cm)	Sample density (g/cm^3)	Erosion rate (cm/yr)	Topographic shielding factor	Production[b] rate	Be AMS standard	Lal (1991)/Stone (2000) constant prod. rate exposure age (ka)	1σ[c] internal (ka)	1σ[d] external (ka)
Little Cottonwood																
Left Lateral	LCL-1	1695	40.57045	111.79414	1.98E+05	6.74E+03	1.09	3.0	2.65	0.0003	0.99550	15.69	07KNSTD	12.8	0.5	1.2
	LCL-2	1714	40.57008	111.79173	2.61E+05	1.11E+04	0.87	1.5	2.65	0.0003	0.99242	16.05	07KNSTD	16.7	0.7	1.7
	LCL-4	1711	40.57039	111.79382	4.07E+05	1.92E+04	0.57	6.0	2.65	0.0003	0.99187	15.43	KNSTD	25.0	1.3	2.6
	LCL-5B	1709	40.57016	111.79189	1.62E+05	5.58E+03	1.01	4.0	2.65	0.0003	0.99217	15.66	07KNSTD	10.4	0.4	1.0
	LCL-6	1706	40.57016	111.79222	2.29E+05	1.10E+04	0.59	2.5	2.65	0.0003	0.99470	15.86	07KNSTD	14.7	0.7	1.5
	LCL-7	1704	40.57023	111.79247	3.21E+05	1.47E+04	0.63	3.5	2.65	0.0003	0.99499	15.71	07KNSTD	21.2	1.0	2.2
	LCL-9	1699	40.57029	111.79267	2.18E+05	1.09E+04	0.68	2.5	2.65	0.0003	0.99638	15.81	07KNSTD	14.1	0.7	1.5
														Mean ± 1σ (n = 7) = 16.4 ± 5.1 ka		
														Error-weighted mean (95% confidence, n = 7, MSWD = 38) = 13.4 ± 3.4 ka		
Right Lateral	02-UT-LCC-01	1584	40.58230	111.79730	2.54E+05	8.14E+03	1.5	3.0	2.65	0.0003	0.99809	14.52	KNSTD	16.2	0.5	1.6
	02-UT-LCC-02	1612	40.58150	111.79380	2.47E+05	6.67E+03	1.5	1.8	2.65	0.0003	0.99720	14.95	KNSTD	15.2	0.4	1.4
	02-UT-LCC-04	1601	40.58280	111.79370	2.49E+05	6.21E+03	1.6	2.0	2.65	0.0003	0.99727	14.81	KNSTD	15.5	0.4	1.5
	02-UT-LCC-05	1605	40.58280	111.79340	2.62E+05	6.55E+03	2.1	3.0	2.65	0.0003	0.99741	14.73	KNSTD	16.4	0.4	1.6
	02-UT-LCC-06	1605	40.58170	111.79480	2.44E+05	6.11E+03	0.8	2.0	2.65	0.0003	0.99789	14.86	KNSTD	15.1	0.4	1.4
	02-UT-LCC-07	1605	40.58230	111.79310	2.44E+05	6.34E+03	1.1	2.0	2.65	0.0003	0.99710	14.85	KNSTD	15.1	0.4	1.4
	02-UT-LCC-08	1611	40.58080	111.79350	2.71E+05	7.04E+03	1.5	2.0	2.65	0.0003	0.99728	14.92	KNSTD	16.8	0.5	1.6
														Mean ± 1σ (n = 7) = 15.7 ± 0.7 ka		
														Error-weighted mean (95% confidence, n = 7, MSWD = 2.5) = 15.7 ± 0.7 ka		
American Fork																
	AF-1	2296	40.52000	111.61967	3.95E+05	1.44E+04	0.70	6.0	2.65	0	0.9860	22.93	KNSTD	15.4	0.6	1.5
	AF-2	2312	40.51835	111.62082	3.91E+05	1.69E+04	0.50	3.0	2.65	0	0.9944	23.95	KNSTD	14.6	0.6	1.4
	AF-3	2313	40.51767	111.62082	4.75E+05	1.90E+04	0.85	4.0	2.65	0	0.9948	23.78	KNSTD	17.8	0.7	1.7
	AF-4	2312	40.51792	111.62115	4.53E+05	1.23E+04	0.45	2.5	2.65	0	0.9932	24.02	KNSTD	16.9	0.5	1.5
	AF-6	2318	40.51932	111.62060	3.90E+05	3.04E+04	1.00	4.0	2.65	0	0.9921	23.80	KNSTD	14.7	1.1	1.7
	AF-7	2285	40.51595	111.62338	3.38E+05	1.52E+04	1.60	4.0	2.65	0	0.9923	23.29	KNSTD	12.9	0.6	1.3
	AF-8	2295	40.51678	111.62357	4.73E+05	1.78E+04	1.20	4.5	2.65	0	0.9947	23.40	KNSTD	18.1	0.7	1.7
	AF-9	2283	40.51583	111.62357	3.92E+05	1.13E+04	1.10	4.0	2.65	0	0.9944	23.30	KNSTD	15.0	0.4	1.4
	AF-10	2311	40.51852	111.62225	4.01E+05	1.74E+04	0.90	4.5	2.65	0	0.9898	23.54	KNSTD	15.2	0.7	1.5
	AF-11	2311	40.51852	111.62225	3.93E+05	7.97E+03	0.85	4.0	2.65	0	0.9898	23.63	KNSTD	14.9	0.3	1.3
														Mean ± 1σ (n = 10) = 15.5 ± 1.6 ka		
														Error-weighted mean (95% confidence, n = 7, MSWD = 6.8) = 15.4 ± 1.0 ka		

Samples from the Little Cottonwood left-lateral and the American Fork were collected and processed by BJCL, KAR, and RAB; samples from the Little Cottonwood right-lateral were collected by DWM and processed by JCG.

[a] Samples from the Little Cottonwood left-lateral and the American Fork were spiked with a commercially-made ^{9}Be carrier; samples from the Little Cottonwood right-lateral with a ^{9}Be carrier made from a beryl crystal from the Homesake Mine (J. Klein).

[b] Spallation production rate determined by CRONUS online exposure-age calculator, version 2.2 (Balco et al., 2008; http://hess.ess.washington.edu/math/) in atoms g SiO_2^{-1} yr^{-1}. Muogenic production is accounted for in age calculations.

[c] Uncertainty of AMS measurement. Uncertainties of measurements during sample preparation, the Be-half life, and the attenuation of secondary cosmic rays are not included.

[d] Uncertainty of AMS measurement and production rate.

Table 2
Comparison of TCN exposure ages of terminal moraines based on constant and time-dependent production rates.

Sample locale	Sample Id	Lal (1991)/Stone (2000) constant exp. age (ka)[a]	1σ ext. (ka)[b]	Desilets and Zreda (2003)/Desilets et al. (2006)[c] exp. age (ka)	1σ ext. (ka)[b]	Dunai (2001)[c] exp. age (ka)	1σ ext. (ka)[b]	Lifton et al. (2005)[c] exp. age (ka)	1σ ext. (ka)[b]	Lal (1991)/Stone (2000)[c] exp. age (ka)	1σ ext. (ka)[b]
Little Cottonwood											
Left Lateral	LCL-1	12.8	1.2	13.2	1.7	13.2	1.7	13.0	1.4	12.8	1.2
	LCL-2	16.7	1.7	17.0	2.2	16.9	2.2	16.6	1.9	16.5	1.6
	LCL-4	25.0	2.6	25.1	3.4	24.8	3.4	24.5	2.9	24.4	2.5
	LCL-5B	10.4	1.0	10.8	1.4	10.7	1.4	10.5	1.1	10.4	1.0
	LCL-6	14.7	1.5	15.1	2.0	15.1	2.0	14.8	1.7	14.7	1.5
	LCL-7	21.2	2.2	21.4	2.9	21.2	2.8	20.9	2.4	20.8	2.1
	LCL-9	14.1	1.5	14.5	1.9	14.4	1.9	14.2	1.6	14.0	1.4
	Mean ± 13%[d]	16.4 ± 2.1		16.7 ± 2.1		16.6 ± 2.1		16.4 ± 2.1		16.2 ± 2.1	
Right Lateral	02-UT-LCC-01	16.2	1.6	16.6	2.1	16.5	2.1	16.3	1.8	16.1	1.5
	02-UT-LCC-02	15.2	1.4	15.7	2.0	15.6	2.0	15.3	1.6	15.1	1.4
	02-UT-LCC-04	15.5	1.5	15.9	2.0	15.8	2.0	15.6	1.7	15.4	1.4
	02-UT-LCC-05	16.4	1.6	16.9	2.1	16.8	2.1	16.5	1.8	16.3	1.5
	02-UT-LCC-06	15.1	1.4	15.6	2.0	15.5	1.9	15.3	1.6	15.1	1.4
	02-UT-LCC-07	15.1	1.4	15.6	2.0	15.5	1.9	15.3	1.6	15.0	1.4
	02-UT-LCC-08	16.8	1.6	17.2	2.2	17.1	2.2	16.9	1.8	16.6	1.5
	Mean ± 13%[d]	15.7 ± 2.0		16.2 ± 2.0		16.1 ± 2.0		15.9 ± 2.0		15.7 ± 2.0	
American Fork											
	AF-1	15.4	1.5	15.2	1.9	15.2	1.9	14.9	1.6	15.2	1.4
	AF-2	14.6	1.4	14.5	1.8	14.4	1.8	14.1	1.5	14.5	1.4
	AF-3	17.8	1.7	17.5	2.2	17.4	2.2	17.1	1.8	17.6	1.6
	AF-4	16.9	1.5	16.6	2.0	16.5	2.0	16.2	1.7	16.7	1.5
	AF-6	14.7	1.7	14.5	2.1	14.5	2.0	14.2	1.8	14.5	1.7
	AF-7	12.9	1.3	12.9	1.6	12.9	1.6	12.6	1.4	12.9	1.2
	AF-8	18.1	1.7	17.8	2.2	17.7	2.2	17.4	1.8	17.8	1.7
	AF-9	15.0	1.4	14.9	1.8	14.8	1.8	14.6	1.5	14.9	1.3
	AF-10	15.2	1.5	15.1	1.9	15.0	1.9	14.7	1.6	15.1	1.4
	AF-11	14.9	1.3	14.7	1.8	14.7	1.8	14.4	1.5	14.7	1.3
	Mean ± 13%[d]	15.5 ± 2.0		15.4 ± 2.0		15.3 ± 2.0		15.0 ± 2.0		15.4 ± 2.0	

Note: all ages displayed in this table are computed by CRONUS online exposure-age calculator, version 2.2 (Balco et al., 2008; http://hess.ess.washington.edu/math/).

[a] Ages are also shown in the previous table and reported in the text.

[b] Uncertainty of the spallogenic and muogenic production rate and of the AMS measurement.

[c] Ages are based on a time-dependent model of production rate from these sources as reported by Balco et al. (2008; http://hess.ess.washington.edu/math/).

[d] This value is based on an average age error of 13% determined from the scaling methods of Desilets et al. (2003, 2006), which yields the largest age error. It is reported here to demonstrate that mean ^{10}Be exposure ages are significantly younger than the Bonneville highstand regardless of which production-rate model is used.

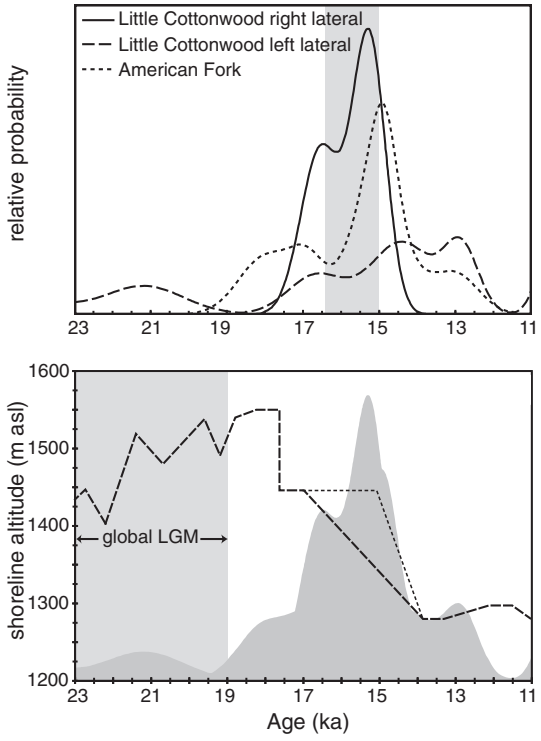

Figure 2. Top: Probability-density plots of TCN ^{10}Be exposure ages for each of the sampled areas; the American Fork moraine and the left- and right-lateral areas of the Little Cottonwood moraine. Mean age, 1σ measurement error, and coefficient of variation (CV) of ages for each moraine are reported in the text and Tables 1 and 2. Curves were computed using all ages from each moraine determined by a constant spallogenic and muogenic production rate and 1σ measurement error, as determined by the CRONUS-Earth online exposure-age calculator, version 2.2 (Balco et al., 2008; http://hess.ess.washington.edu/math/). Light gray area is the estimated time of terminal moraine abandonment in the western Wasatch Mountains, 15.7 ± 1.3 ka. The far right (young) tail of the probability curve for the left-lateral area of the Little Cottonwood moraine is not shown, but the relative probability values for this part of the curve are minimal. Bottom: Probability-density of TCN exposure ages for all three moraines (darker gray) compared to the hydrograph of Lake Bonneville (dashed line; corrected to calendar years from Oviatt, 1997). The dotted line represents the possible revision to the Bonneville hydrograph suggested by Godsey et al. (2005a). Lighter gray area at the left-hand side of the plot represents the latter interval of the global LGM, as limited by Clark et al. (2009).

terminal moraine, which indicates ice retreat by 14.4 ± 0.5 cal ka BP (Madsen and Currey, 1979). Fourth, ^{10}Be surface-exposure ages on moraine boulders in the nearby Uinta Mountains (Laabs et al., 2009; the location of the Uinta Mountains is shown in Fig. 1) determined with the same TCN ^{10}Be production rate used in this study are consistent with radiocarbon-age limits on the start of ice retreat in the Bear River valley (Rosenbaum and Heil, 2009). Together these considerations support the conclusion that ^{10}Be exposure ages for terminal moraines in the western Wasatch Mountains are accurate and indicate the onset of glacier retreat at 15.7 ± 1.3 ka.

Discussion

Deglaciation commenced during or after the Lake Bonneville highstand

Based on the new TCN ^{10}Be exposure ages of terminal moraines reported here, glaciers in the western Wasatch Mountains abandoned their terminal moraines at 15.7 ± 1.3 ka. This timing for the start of deglaciation is consistent with findings in the western Uinta Mountains (Refsnider et al., 2008; Laabs et al., 2009), the Teton Range in Wyoming (Licciardi and Pierce, 2008), some valleys in the Colorado Rocky Mountains (Guido et al., 2007; Briner, 2009; Ward et al., 2009) and some valleys on the northern Yellowstone Plateau (Licciardi and Pierce, 2008), where TCN exposure ages of terminal moraines suggest the start of ice retreat between ca. 17 and 14 ka.

If the production rates and scaling models used to compute the TCN ^{10}Be exposure ages reported here are correct, then comparison of these ages with the radiocarbon-based hydrograph of Lake Bonneville (Fig. 2) indicates that deglaciation commenced when Lake Bonneville occupied (and likely overflowed at) the Provo shoreline (~1450 m asl). This finding warrants some discussion of the relatively small volume of the terminal moraine at Little Cottonwood Canyon, at least when compared to the size of the glacier that occupied the canyon (it was the largest in the Wasatch Mountains during the Pinedale Glaciation) and the comparatively voluminous moraine deposited by the much smaller glacier that occupied Bells Canyon immediately to the south. Previous reports, including the original study of Gilbert (1890), note this discrepancy and suggest that a portion of the terminal moraine at Little Cottonwood Canyon was washed away by waves along the eastern shore of Lake Bonneville. However, the TCN ^{10}Be exposure ages reported here, at least from the right-lateral sector of the terminal moraine, suggest this was not the case. Ice dynamics in Little Cottonwood Canyon may explain the relatively small size of the terminal moraines at its mouth. For example, supraglacial sediment production on the north side of the canyon, which displays lesser slope angles and hosted fewer tributary glaciers than the south side of the canyon (Richmond, 1964), may have been less than on the south side, resulting in greater till deposition rates on the south side of the canyon (at the left-lateral moraine) compared to the north side (at the right-lateral moraine). Another possibility is that variable ice accumulation and ablation rates in the canyon resulted in a fluctuating glacier terminus position, thereby minimizing the time of deposition of the terminal moraine. A third possibility is based on the variability of TCN ^{10}Be exposure ages from the left-lateral sector of the terminal moraine and the stratigraphic observation of shoreline gravel overlying the distal slope of the terminal moraine at Bells Canyon (Richmond, 1964; Scott and Shroba, 1985; Personius and Scott, 1992). As noted above, the left-lateral sector has high relief (greater than 60 m) compared to the right-lateral sector of the terminal moraine (less than 20 m), and does not appear to grade to an end moraine loop that would connect it to the right-lateral moraine. Instead, the morphology of the left-lateral moraine is similar to the latero-frontal terminal moraine at Bells Canyon, the distal slope of which is overlain by shoreline gravels of Lake Bonneville. Given the broad scatter of TCN ^{10}Be exposure ages from the left-lateral moraine at Little Cottonwood Canyon, this moraine may have been deposited prior to the Lake Bonneville highstand. This interpretation is possible if the oldest TCN ^{10}Be exposure ages from this moraine (25.0 ± 1.3 ka, 21.2 ± 1.0 ka) provide the best estimate for the time of moraine abandonment. If so, then the distal portion of the left-lateral moraine may have been washed away by waves along the eastern shore of Lake Bonneville as previous reports have suggested (Gilbert, 1890). Finally, the geomorphic dissimilarity between the left-lateral and right-lateral sectors of the terminal moraine at Little Cottonwood Canyon allow for the possibility that the right-lateral sector was deposited during a short-lived advance (or readvance) to the canyon mouth in which the glacier was too thin near its margin to reoccupy the crest of the left-lateral moraine. Further testing is needed to evaluate this explanation, but it is consistent with previous observations that suggest ice occupation of the mouth of Little Cottonwood Canyon prior to the Lake Bonneville highstand, which is discussed further below.

Reconciling TCN ^{10}Be exposure ages of terminal moraines with previous stratigraphic observations at the western Wasatch Front

The basis for previous suggestions that deglaciation commenced prior to the Lake Bonneville highstand includes stratigraphic observations at the western front of the Wasatch Mountains. Close consideration of the context of these stratigraphic observations can reconcile them with TCN ^{10}Be exposure ages of terminal moraines

Table 3
Reconstructed glacier equilibrium-line altitudes in Northern Utah and Nevada.

Number	Mountains[a]	Drainage	ELA (m asl)		Average ELA (m asl)	1σ
			Toe–headwall altitude ratio[b]	Accumulation-area ratio[c]		
1	Independence	Foreman Ck	2369	2469	2419	71
2		Chicken Creek	2388	2438	2413	36
3		Pratt Creek	2491	2573	2532	58
4		Pratt Creek Trib	2649	2658	2654	6
5		Mill Creek	2494	2560	2527	47
6		North Fork Pratt Ck	2512	2487	2500	18
7		Walker Ck	2410	2536	2473	89
8		McAfee Ck	2491	2633	2562	101
9		Peterson Ck	2517	2560	2539	31
10		Sammy Ck	2382	2426	2404	31
11		Beadles Ck	2395	2512	2453	82
12		Rim Ck	2448	2475	2462	19
13		Dry Canyon	2395	2536	2466	100
14	Ruby	Cave Creek Canyon South	2873	2853	2863	14
15		Cass House Peak	2687	2719	2703	22
16		Cave Creek Canyon	2820	2829	2824	6
17		Pearl Peak South 3	3027	3036	3032	6
18		Cass House Peak North	2776	2853	2814	55
19		Pearl Peak South 2	2972	2987	2979	11
20		Pearl Peak South 1	2745	2853	2799	76
21		Pearl Peak North	2728	2768	2748	28
22		Pearl Lake East	2734	2896	2815	114
23		Pearl Lake	2761	2853	2807	65
24		Pearl Lake North	2781	2804	2793	16
25		Green Mountain South	2840	2902	2871	44
26		Hankins Creek	2731	2816	2774	60
27		McCutcheon Creek South	2647	2774	2710	90
28		Dawley Canyon	2550	2621	2585	51
29		South Fork Smith Creek	2651	2755	2703	74
30		McCutcheon Creek North	2667	2731	2699	45
31		Tipton Canyon	2726	2725	2725	0
32		Middle Fork Smith Creek	2662	2670	2666	5
33		Mayhew Creek South	2715	2749	2732	24
34		Mayhew Creek Middle	2674	2743	2709	49
35		Mayhew Creek North	2670	2694	2682	17
36		North Fork Smith Creek	2696	2829	2762	93
37		Overland Creek	2615	2780	2697	116
38		Rattlesnake Canyon	2464	2804	2634	240
39		North Fork Smith Creek North	2673	2621	2647	37
40		Gennette Creek	2518	2682	2600	116
41		Little Cottonwood Creek	2434	2438	2436	3
42		Little Overland West	2638	2719	2678	57
43		Cottonwood Creek	2424	2469	2447	31
44		Little Overland Middle	2749	2755	2752	4
45		Little Overland East	2858	2865	2861	5
46		Overland Creek North 1	2711	2804	2758	66
47		Overland Creek North 2	2676	2694	2685	13
48		Long Canyon	2475	2804	2640	233
49		Segunda Creek	2493	2743	2618	177
50		Little Rattlesnake East	2672	2792	2732	84
51		Little Rattlesnake West	2782	2804	2793	16
52		Myers Creek South	2801	2950	2876	106
53		Myers Creek North	2705	2774	2739	49
54		Battle Creek South	2689	2829	2759	99
55		Mahogany Creek	2653	2621	2637	22
56		Battle Creek North	2756	2804	2780	34
57		Gedney Creek	2615	2694	2655	56
58		Carter Creek	2591	2609	2600	13
59		Wines Creek	2611	2621	2616	8
60		North Furlong Creek	2562	2755	2659	137
61		Lake Peak SE	2707	2755	2731	34
62		Lake Peak E	2799	2835	2817	25
63		Kleckner Creek	2570	2804	2687	166
64		Colonel Moore Creek	2783	2896	2840	79
65		Lamoille	2637	2896	2766	183
66		Box Canyon	2623	2768	2695	102
67		Thompson Creek South	2682	2743	2713	43
68		Thompson Creek North	2717	2865	2791	105
69		Thomas Canyon	2599	2926	2763	231
70		Right Hand Fork Lamoille	2515	2694	2605	127
71		Echo Canyon	2637	2835	2736	140
72		Seitz-Hennan	2433	2743	2588	219
73		Lutz Creek South	2626	2841	2733	152

(continued on next page)

Table 3 (*continued*)

Number	Mountains[a]	Drainage	ELA (m asl)		Average ELA (m asl)	1σ
			Toe–headwall altitude ratio[b]	Accumulation-area ratio[c]		
74		Young Creek	2493	2707	2600	151
75		Noon Rock	2375	2512	2443	97
76		Lutz Creek Middle	2713	2768	2740	38
77		Verdi Peak Southeast	2779	2829	2804	35
78		Right Hand Fork Lamoille West 1	2766	2877	2822	79
79		Thomas Fork West 1	2858	2890	2874	22
80		Thomas Fork West 2	2659	2694	2677	25
81		Thomas Fork West 3	2530	2585	2558	38
82		Right Hand Fork Lamoille West 2	2564	2902	2733	239
83		Talbot Creek	2509	2865	2687	252
84		Verdi Peak East	2897	2926	2911	21
85		Verdi Peak Northeast	2885	2926	2905	29
86		Lamoille Creek Northeast Trib 2	2678	2792	2735	81
87		Lutts Creek North	2738	2804	2771	47
88		Lamoille Creek Northeast Trib 1	2713	2835	2774	86
89		Lamoille Creek North-Central Trib	2790	2804	2797	10
90		Lamoille Creek Northwest Trib	2661	2792	2726	93
91		Smith Peak East	2753	2743	2748	7
92		Talbot Creek Trib	2546	2755	2651	148
93		Thorpe Creek	2631	2719	2675	62
94		North Smith Creek	2702	2719	2710	12
95		Conrad Creek	2589	2682	2636	66
96		Dads Creek South	2702	2816	2759	81
97		Dads Creek Middle	2723	2755	2739	23
98		Thorpe Creek North	2674	2865	2770	135
99		Dads Creek North 2	2532	2524	2528	6
100		Dads Creek North 1	2705	2731	2718	18
101		Griswold Creek South	2736	2841	2789	74
102		Griswold Creek North	2621	2890	2755	190
103		South Fork Cold Creek	2718	2780	2749	44
104		Middle Fork Cold Creek	2646	2780	2713	94
105		Withington Canyon	2635	2725	2680	64
106		Soldier Creek	2646	2755	2701	78
107		North Fork Cold Creek	2668	2743	2706	53
108		John Day Canyon	2761	2816	2789	39
109		John Day Peak NE	2799	2829	2814	21
110		John Day Peak N	2791	2829	2810	26
111		John Day Cirque	2756	2829	2792	51
112		John Day Peak NW	2651	2707	2679	39
113		Sharps Creek	2546	2573	2559	19
114		Sharps Creek N	2545	2573	2559	19
115		Soldier Peak S	2710	2743	2726	24
116		Soldier Peak SW 1	2711	2719	2715	6
117		Soldier Peak SW 2	2649	2682	2665	24
118		Soldier Peak SW 3	2543	2682	2612	99
119		Krenka Creek	2466	2548	2507	58
120		Ross Creek	2515	2609	2562	67
121		Soldier Peak SW 4	2460	2585	2523	88
122		Wilson Creek	2643	2755	2699	79
123		Soldier Peak SW 5	2418	2426	2422	6
124		Franklin River	2480	2518	2499	26
125		Soldier Peak North	2562	2597	2579	25
126		Murphy Creek	2440	2484	2462	31
127		Secret Peak South	2418	2451	2434	23
128		Secret Peak NE	2391	2402	2396	8
129		Secret Peak NW	2333	2377	2355	31
130	East Humboldt	Pole Canyon	2597	2682	2640	60
131		Johnson Creek	2451	2524	2487	52
132		Second Boulder Creek	2548	2743	2646	138
133		South Fork Steele Creek	2609	2719	2664	78
134		Third Boulder Creek	2591	2829	2710	168
135		Steele Creek	2609	2719	2664	78
136		Weeks Creek	2560	2652	2606	65
137		Fourth Boulder Creek	2505	2646	2576	99
138		Leach Creek	2676	2621	2649	39
139		South Ackler Creek	2597	2694	2646	69
140		Ackler Creek	2609	2646	2627	26
141		Winchell Creek	2573	2560	2566	9
142		South Fork Herder Creek	2457	2463	2460	4
143		Wiseman Creek	2621	2560	2591	43
144		Middle Fork Herder Creek	2460	2499	2480	28
145		Schoer Creek	2688	2682	2685	4
146		South Fork Angel Creek	2737	2719	2728	13
147		North Herder Creek	2497	2524	2510	19
148		North Fork Angel Creek	2585	2621	2603	26

Table 3 (*continued*)

Number	Mountains[a]	Drainage	ELA (m asl)		Average ELA (m asl)	1σ
			Toe–headwall altitude ratio[b]	Accumulation-area ratio[c]		
149		Grays Creek	2451	2536	2493	60
150		Clover Creek	2512	2475	2493	26
151		Trout Creek	2475	2499	2487	17
152	Deep Creek	Haystack Peak	3021	3170	3096	105
153		Red Cedar Creek	2951	3206	3079	181
154		Steves Creek North	2793	2804	2798	8
155		Steves Creek South	2834	2816	2825	13
156		Granite Creek	3078	3194	3136	82
157	Stansbury	Pass Canyon	2570	2606	2588	26
158		Little Pole Canyon	2692	2719	2705	19
159		North Willow	2488	2597	2542	77
160		Big Pole Canyon	2732	2658	2695	52
161		Mining fork	2441	2560	2500	85
162		Spring Canyon	2713	2719	2716	4
163		South Willow Canyon	2422	2606	2514	130
164		Big Creek Canyon	2692	2707	2699	10
165	Oquirrh	Settlement Canyon	2750	2804	2777	38
166		Lowe Canyon	2654	2658	2656	3
167		Jackson Hollow	2675	2755	2715	57
168		Jumpoff	2590	2606	2598	11
169	Wasatch	American	2567	2560	2564	5
170		Little Cottonwood	2141	2606	2374	329
171		Bells	2221	2713	2467	348
172		Silver lake	2610	2682	2646	51
173		Dry creek	2226	2652	2439	301
174	Uinta[d]	Heber Mountain	2403	2469	2436	47
175		Pinon Canyon	2610	2621	2616	8
176		Swifts Canyon	2520	2682	2601	115
177		Bear Basin	2524	2524	2524	0
178		White Pine	2570	2667	2619	69
179		South Fork	2610	2774	2692	116
180		Nobletts Creek	2680	2646	2663	24
181		Shingle Mil	2670	2743	2707	52
182		Shingle Mill East	2700	2633	2667	47
183		Bear Trap North	2770	2768	2769	1
184		Smith & Morehouse	2710	2880	2795	120
185		Slader Ridge West	2700	2719	2710	13
186		Broad Canyon	2800	2725	2763	53
187		Slader Creek	2770	2728	2749	30
188		Main Weber	2780	2972	2876	136
189		West Fork Bear River	2788	2880	2834	65
190		Gold Hill	2888	2840	2864	34
191		Duchesne	2719	3005	2862	202
192		Hayden Fork Bear River	2948	3025	2987	54
193		East Fork Bear River	2988	3035	3012	33
194		Log Hollow	2904	3008	2956	74
195		Rock Creek	2733	3132	2933	282
196		Little West Fork Blacks Fork	2952	2990	2971	27
197		Blacks Fork	3036	3020	3028	11
198		Lake Fork	2881	3170	3026	204
199		West Fork Smiths Fork	3136	3110	3123	18
200		Smiths Fork	3080	3045	3063	25
201		Yellowstone	2811	3185	2998	264
202		Henrys Fork	3112	3130	3121	13
203		West Fork Beaver Creek	3156	3230	3193	52
204		Crow Canyon	3075	3078	3077	2
205		Heller Lake	3019	3011	3015	6
206		Middle Fork Beaver Creek	3168	3210	3189	30
207		Thompson Creek	3084	3125	3105	29
208		Uinta	2853	3286	3070	306
209		Burnt Fork	3048	3210	3129	115
210		Upper Rock Lake	2980	3089	3035	77
211		Middle Fork Sheep Creek*	3128	3130	3129	1
212		Whiterocks	2755	3267	3011	362
213		South Fork Sheep Creek*	3068	3170	3119	72
214		West Fork Carter Creek*	3068	3140	3104	51
215		Dry Fork	2897	3093	2995	139
216		East Fork Carter Creek*	3048	3060	3054	8
217		North Fork Ashley	3136	3160	3148	17
218		Chimney Rock Lake	3116	3097	3107	13
219		South Fork Ashley*	3040	3100	3070	42

[a] Mountains ranges are listed from west to east.
[b] Toe–headwall altitude ratio = 0.35(highest headwall altitude − toe altitude) + toe altitude.
[c] Assumed ratio accumulation-area ratio of 0.65. If flagged by * symbol, then assumed accumulation area ratio of 0.5.
[d] Data are from Munroe and Mickelson (2002) and Laabs and Carson (2005).

reported here. All previous reports of shoreline gravels of Lake Bonneville overlying till mapped as Pinedale-equivalent (Madsen and Currey, 1979; Scott et al., 1983) include only broad age limits on the time between deposition of till and the overlying shoreline gravels. Although the timing of the Lake Bonneville highstand is well established, the age of the underlying till is limited only by its weathering characteristics (Scott et al., 1983) and by correlations to nearby settings where age limits are available (Madsen and Currey, 1979). Additionally, some recent reports include observations of till *overlying* shoreline gravels of Lake Bonneville at the western front of the Wasatch Mountains (Personius and Scott, 1992; Godsey et al., 2005b), thereby indicating multiple ice advances to the mouth of Little Cottonwood Canyon. However, as noted above, whether the till underlying shoreline gravels was deposited during MIS 2 or an earlier interval of the late Pleistocene cannot be discerned from the available data.

An alternative interpretive model, one that requires additional testing, combines previous stratigraphic observations at the western front of the Wasatch Mountains, the most recent chronology of Lake Bonneville, and the ^{10}Be exposure ages for terminal moraines reported here, and is similar to the conclusion of Licciardi et al. (2004) that two mountain glacier maxima occurred during the last Pleistocene glaciation in the western U.S. In the western Wasatch Mountains, this may include one maximum prior to 21.3 ka (but during MIS 2) and another involving the construction of the preserved terminal moraines, ending at 15.7 ± 1.3 ka. While it is not possible to determine from available evidence when the first glacial maximum began, if the pedo-stratigraphic observation of Scott et al. (1983) is accurate, then the weakly weathered Pinedale-equivalent till buried by shoreline gravel of Lake Bonneville indicates ice presence at the canyon mouth prior to ca. 21.3 ka. A glacier maximum at this time is consistent with the timing of maxima in the western Uinta Mountains, 20 to 19 cal ka BP as established by radiocarbon ages of glacial flour deposited in Bear Lake (Rosenbaum and Heil, 2009). Additionally, this maximum would have been synchronous with mountain glacier maxima in the Wind River Range, Wyoming (Gosse et al., 1995), the Colorado Rocky Mountains (e.g., Benson et al., 2005; Brugger, 2007), the northwestern Colorado Plateau (Marchetti et al., 2005) and the global Last Glacial Maximum at 26.5 to 19 ka (Clark et al., 2009). If the glacier in Little Cottonwood Canyon deposited a terminal moraine prior to the Bonneville highstand, then the moraine may have been eroded away by wave action along the shore of Lake Bonneville (as suggested by previous studies), and the remnant of this moraine may be the Pinedale-equivalent till that extends beyond the terminal moraines at the mouth of the canyon. If the stratigraphic observations of Godsey et al. (2005b) are accurate, the glacier then deposited the right-lateral sector of the terminal moraine after the Bonneville highstand (and above its shoreline elevation of ~1550 m asl) before beginning its final retreat. Based on glacial geomorphic evidence at American Fork Canyon, it is unclear whether the glacier would have persisted at the terminal moraine during the Bonneville highstand (18.7 to 17.6 cal ka BP) or readvanced to the terminal moraine prior to 15.7 ± 1.3 ka; the former seems more likely considering that mountain glaciers occupied terminal moraines in the nearby Uinta Mountains during this time (Laabs et al., 2009).

Paleoclimatic significance

The results of this and other studies (e.g., Licciardi et al., 2004; Laabs et al., 2009) challenge the long-standing view that mountain glaciers in the Great Basin abandoned their terminal moraines prior to the highstands of Great Basin paleolakes, and instead support the theory that climate during the last glaciation in the interior western U.S. favored nearly synchronous expansion of glaciers and lakes. While some studies have characterized the climate in the vicinity of Lake Bonneville during MIS 2 (24 to 12 ka) as cold and dry (e.g., Galloway, 1970; Kaufman, 2003) with less-than-modern precipitation, other studies have concluded that greater-than-modern precipitation accompanied paleolake maxima (Benson and Thompson, 1987; Hostetler et al., 1994). For Lake Bonneville, its maxima spans the time interval during which it overflowed at the Bonneville and Provo shorelines (18.7 to 15.0 cal ka BP).

The potential relationship between Great Basin paleolakes and nearby mountain glaciers can be explored by reconstructing the regional pattern of mountain glacier equilibrium-line altitudes (ELAs) across northeastern Nevada and Utah. The ELAs reported here are based on an assumed accumulation-area ratio of 0.65 (0.5 for piedmont glaciers) and a toe–headwall altitude ratio of 0.35 (Table 3). Meierding (1982) concluded that these two methods of estimating ELAs of Pleistocene mountain glaciers yield the lowest error when compared to other methods, although a subsequent study by Torsnes et al. (1993) determined that the accumulation-area ratio method is accurate to ~20 m asl for ELA reconstructions whereas the toe–headwall altitude ratio is accurate to ~200 m. Therefore, the regional pattern of mountain glaciation is characterized here based on the mean ELA determined by both methods and the ELA based on only accumulation-area ratio (Fig. 3).

The pattern of mountain glaciation in the northeastern Great Basin suggests that paleolakes affected the mass balance of mountain glaciers in the region. Reconstructed ELAs in northern Nevada (west of Lake Bonneville) and northern Utah are higher at the western (upwind) end of the Bonneville Basin, decline markedly west-to-east across the region inundated by the paleolake, and rise steeply eastward beginning at the

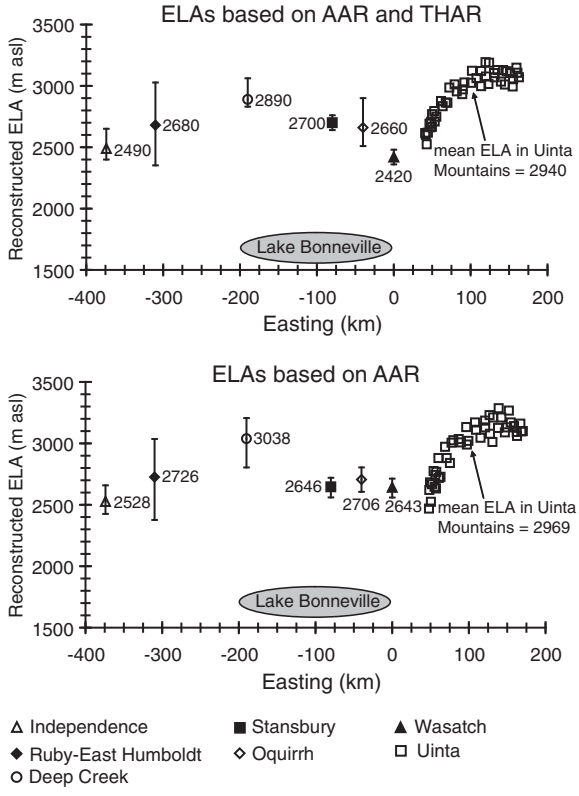

Figure 3. Reconstructed glacier ELAs during the last glaciation for several mountain ranges at ~N40° to N41° along a west-to-east transect across northern Utah and northeastern Nevada (for Independence, n = 13 glaciers; Ruby-East Humboldt, n = 138; Deep Creek, n = 5; Stansbury, n = 8; Oquirrh, n = 4; western Wasatch, n = 5; Uinta, n = 44). The lower plot displays ELAs determined by accumulation-area ratio and the upper by the average of estimates determined by the accumulation-ratio and toe–headwall altitude ratio. Individual ELAs and calculation methods are described in the text and given in Table 3. ELAs of individual valley glaciers in the Uinta Mountains (Munroe et al., 2006) are shown at the right-hand side of the plot to illustrate the rise in glacier ELA east (and downwind) of the Wasatch Mountains. The extent of Lake Bonneville (maximum lake surface elevation of 1550 m asl) is indicated by the gray oval.

Wasatch Mountains and continuing into the Uinta Mountains (Fig. 3; Table 3). This ELA pattern is not mirrored by the modern winter precipitation distribution in the region; instead, January precipitation at altitude ca. 2750 m asl (the mean paleo-glacier ELA in the region) actually declines in mountain ranges from northeastern Nevada to the western front of the Wasatch Mountains (PRISM Climate Group; http://www.prism.oregonstate.edu). However, the ELA pattern provides strong evidence for increasing moisture availability toward the eastern shore of Lake Bonneville, as reported in previous studies of glaciation in northern Utah (Munroe and Mickelson, 2002; Munroe et al., 2006). Thus, the persistence of some mountain glacier maxima for ~4 ka after the start of the northern hemisphere deglaciation (at 19 ka) may reflect a combined response to both the precipitation increase that drove paleolake maxima and local precipitation enhancement downwind from paleolakes.

Conclusions

On the basis of the TCN ^{10}Be exposure ages of terminal moraines reported here, deglaciation in Little Cottonwood and American Fork Canyons in the western Wasatch Mountains commenced at 15.7 ± 1.3 ka either during or shortly after the Lake Bonneville highstand. This finding is inconsistent with some (but not all) previous stratigraphic observations of shoreline gravels of Lake Bonneville overlying till at the western front of the Wasatch Mountains, but does not overrule these observations. Instead, it is consistent with previous suggestions that deposition of till at mouth of Little Cottonwood Canyon during the Pinedale Glaciation occurred during multiple ice advances. Deglaciation commencing at 15.7 ± 1.3 ka is also consistent with numerous Pinedale glacial chronologies from elsewhere in the Middle and Southern Rocky Mountains, and with other latest Pleistocene glacier chronologies from elsewhere in the northern and southern hemispheres (Schaefer et al., 2006). Whether ice occupied the mouth of Little Cottonwood Canyon before and after the Lake Bonneville highstand during MIS 2 remains equivocal, but could be resolved by additional dating of moraines (especially the terminal moraine at Bells Canyon) and other locales in the western Wasatch Mountains.

Although the growing body of data supporting a delayed start of mountain glacier retreat relative to the retreat of the Laurentide Ice Sheet has prompted inferences of the relative impacts of temperature and precipitation changes in the western U.S. during the last deglaciation (e.g., Licciardi et al., 2004; Thackray et al., 2004), the forcings and magnitudes of these changes remain largely unclear. Records from mid-latitudes in the Pacific (e.g., Mix et al., 1999) and high latitudes in the North Atlantic (Stuiver and Grootes, 2000) suggest that temperatures in these regions remained low (at glacial levels) until about 15 ka, as do temperature reconstructions for the Lake Bonneville basin (Kaufman, 2003), whereas Schaefer et al. (2006) suggest that rising atmospheric carbon dioxide levels and warm summers initiated global deglaciation at 17 ka. The development of high-resolution, terrestrial paleotemperature reconstructions for this interval in combination with modeling of glacier and paleolake responses to temperature and precipitation changes (e.g., Blard et al., 2009) can improve the understanding of latest Pleistocene climate change in the western U.S.

Acknowledgments

The authors thank the following people for assistance with this research: M. Caffee and others at PRIME Lab; G. Yang at Dalhousie University, R. Finkel at the CAMS-Lawrence Livermore National Laboratory; J. Jahnz at the University of Wisconsin; K. Lawson and A. Rishavy at Gustavus Adolphus College. The authors also thank A. Gillespie, K. Adams, C. (Jack) Oviatt and one anonymous reviewer for helpful comments on the original draft of this paper. This research was supported by the U.S. National Science Foundation grant EAR-0345277.

References

Adams, K.D., Wesnousky, S.G., 1998. Shoreline processes and the age of the Lake Lahontan highstand in the Jessup embayment, Nevada. Geological Society of America Bulletin 10, 1318–1332.
Applegate, P.J., Urban, N.M., Laabs, B.J.C., Keller, K., Alley, R.B., 2010. Modeling the statistical distributions of cosmogenic exposure dates from moraines. Geoscientific Model Development 3, 293–307.
Balco, G., Stone, J., Lifton, N., Dunai, T., 2008. A complete and easily accessible means of calculating surface exposure ages or erosion rates from ^{10}Be and ^{26}Al measurements. Quaternary Geochronology 3, 174–195.
Benson, L., Madole, R., Landis, G., Gosse, J., 2005. New data for late Pleistocene Pinedale alpine glaciation from southwestern Colorado. Quaternary Science Reviews 24, 49–65.
Benson, L.V., Currey, D.R., Dorn, R.I., Lajoie, K.R., Oviatt, C.G., Robinson, S.W., Smith, G.I., Stine, S., 1990. Chronology of expansion and contraction of four Great Basin lake systems during the past 35,000 years. Palaeogeography, Palaeoclimatology, Palaeoecology 78, 241–286.
Benson, L.V., Thompson, R.S., 1987. The physical record of lakes in the Great Basin. North American and adjacent oceans during the last deglaciation. : In: Ruddiman, W.F., Wright Jr., H.E. (Eds.), The Geology of North America, L. Geological Society of America, Boulder, Colorado, pp. 241–260.
Bierman, P.R., Caffee, M.W., Davis, P.T., Marsella, K., Pavich, M., Colgan, P., Mickelson, D., Larsen, J., 2002. Rates and timing of Earth-surface processes from *in situ*-produced cosmogenic Be-10. Beryllium: Mineralogy, Petrology and Geochemistry: In: Grew, E.S. (Ed.), Reviews in Mineralogy and Geochemistry, 50, pp. 147–205.
Blard, P.-H., Lavé, J., Farley, K.A., Fornari, M., Jiménez, N., Ramirez, V., 2009. Late local glacial maximum in the Central Altiplano triggered by cold and locally-wet conditions during the paleolake Tauca episode (17–15 ka, Heinrich 1). Quaternary Science Reviews 28, 3414–3427.
Broecker, W.S., Kaufman, A., 1965. Radiocarbon chronology of Lake Lahontan and Lake Bonneville II, Great Basin. Geological Society of America Bulletin 76, 537–566.
Briner, J.P., 2009. Moraine pebbles and boulders yield indistinguishable 10Be ages: a case study from Colorado, U.S.A. Quaternary Geochronology 4, 299–305.
Brugger, K.A., 2007. Cosmogenic 10Be and 36Cl ages from late Pleistocene terminal moraine complexes in the Taylor River drainage basin, central Colorado, U.S.A. Quaternary Science Reviews 26, 494–499.
Bryant, B., 1992. Geologic and structure maps of the Salt Lake City 1°×2° quadrangle, Utah and Wyoming. U.S. Geological Survey Miscellaneous Investigations Series Map, I-1997: 1:125,000 scale.
Clark, P.U., Dyke, A.S., Shakun, J.D., Carlson, A.E., Clark, J., Wohlfarth, B., Mitrovica, J.X., Hostetler, S.W., McCabe, A.M., 2009. The Last Glacial Maximum. Science 325, 710–714.
Desilets, D., Zreda, M., 2003. Spatial and temporal distribution of secondary cosmic-ray nucleon intensities and applications to in-situ cosmogenic dating. Earth and Planetary Science Letters 206, 21–42.
Desilets, D., Zreda, M., Prabu, T., 2006. Extended scaling factors for in situ cosmogenic nuclides: new measurements at low latitude. Earth and Planetary Science Letters 246, 265–276.
Douglass, D.C., Singer, B.S., Kaplan, M.R., Mickelson, D.M., Caffee, M.W., 2006. Cosmogenic nuclide surface exposure dating of boulders on last-glacial and late-glacial moraines, Lago Buenos Aires, Argentina; interpretive strategies and paleoclimate implications. Quaternary Geochronology 1, 43–58.
Dunai, T., 2001. Influence of secular variation of the magnetic field on production rates of in situ produced cosmogenic nuclides. Earth and Planetary Science Letters 193, 197–212.
Galloway, R.W., 1970. The full-glacial climate of the southwestern United States. Annals of the Association of American Geographers 60, 245–256.
Gilbert, G.K., 1890. Lake Bonneville. U. S. Geological Survey Monograph, 1. 438 pp.
Godsey, H.S., Currey, D.R., Chan, M.A., 2005a. New evidence for an extended occupation of the Provo shoreline and implications for regional climate change, Pleistocene Lake Bonneville, Utah, USA. Quaternary Research 63, 212–223.
Godsey, H.S., Atwood, G., Lips, E., Miller, D.M., Milligan, M., Oviatt, C.G., 2005b. Don R. Currey Memorial Field Trip to the shores of Pleistocene Lake Bonneville. Interior Western United States: In: Pederson, J., Dehler, C.M. (Eds.), Geological Society of America Field Trip Guide, 6, pp. 419–448.
Gosse, J.C., Klein, J., Evenson, E.B., Lawn, B., Middleton, R., 1995. Beryllium-10 dating of the duration and retreat of the last Pinedale glacial sequence. Science 268, 1329–1333.
Gosse, J.C., Phillips, F.M., 2001. Terrestrial in situ cosmogenic nuclides; theory and application. Quaternary Science Reviews 20, 1475–1560.
Guido, Z.S., Ward, D.J., Anderson, R.S., 2007. Pacing the post-Last Glacial Maximum demise of the Animas Valley glacier and the San Juan Mountain ice cap, Colorado. Geology 35, 739–742.
Hostetler, S.W., Giorgi, F., Bates, G.T., Bartlein, P.J., 1994. Lake-atmosphere feedbacks associated with paleolakes Bonneville and Lahontan. Science 263, 665–668.
Kaufman, D.S., 2003. Amino acid paleothermometry of Quaternary ostracodes from the Bonneville Basin, Utah. Quaternary Science Reviews 22, 899–914.
Laabs, B.J.C., Refsnider, K.A., Munroe, J.S., Mickelson, D.M., Applegate, P.A., Singer, B.S., Caffee, M.W., 2009. Latest Pleistocene glacial chronology of the Uinta Mountains: support for moisture-driven asynchrony of the last deglaciation. Quaternary Science Reviews 28, 1171–1187.
Laabs, B.J.C., Carson, E.C., 2005. Glacial geology of the southern Uinta Mountains. Uinta Mountain geology: In: Dehler, C.M., Pederson, J.L., Sprinkel, D.A., Kowallis, B.J. (Eds.), Utah Geological Association Monograph, 33, pp. 235–254.
Lal, D., 1991. Cosmic ray labeling of erosion surfaces: in situ nuclide production rates and erosion rates. Earth and Planetary Science Letters 104, 424–439.

Licciardi, J.M., Pierce, K.L., 2008. Cosmogenic exposure-age chronologies of Pinedale and Bull Lake glaciations in greater Yellowstone and the Teton Range, USA. Quaternary Science Reviews 27, 814–831.
Licciardi, J.M., Clark, P.U., Brook, E.J., Elmore, D., Sharma, P., 2004. Variable responses of western U.S. glaciers during the last deglaciation. Geology 32, 81–84.
Lifton, N., Bieber, J., Clem, J., Duldig, M., Evenson, P., Humble, J., Pyle, R., 2005. Addressing solar modulation and long-term uncertainties in scaling secondary cosmic rays for in situ cosmogenic nuclide applications. Earth and Planetary Science Letters 239, 140–161.
Madsen, D.B., Currey, D.R., 1979. Late Quaternary glacial and vegetation changes, Little Cottonwood Canyon Area, Wasatch Mountains, Utah. Quaternary Research 12, 254–270.
Marchetti, D.W., Cerling, T.E., Lips, E.W., 2005. A glacial chronology for the Fish Creek drainage of Boulder Mountain, USA. Quaternary Research 64, 263–271.
Meierding, T.C., 1982. Late-Pleistocene glacial equilibrium-line altitudes in the Colorado Front Range; a comparison of methods. Quaternary Research 18, 289–310.
Mix, A.C., Lund, D.C., Pisias, N.G., Bodé, N.P., Born-Malm, L., Lyle, M., Pike, J., 1999. Rapid climate oscillations in the northeast Pacific during the last deglaciation reflect Northern and Southern Hemisphere sources. Mechanisms of global climate change at millennial time scales: In: Clark, P.U., Webb, R.S., Keigwin, L.D. (Eds.), American Geophysical Union Geophysical Monograph, 112, pp. 127–148.
Morrison, R.B., 1965. Lake Bonneville: Quaternary stratigraphy of eastern Jordan Valley, south of Salt Lake City, Utah. U.S. Geological Survey Professional Paper, 447. 80 pp.
Munroe, J.S., Laabs, B.J.C., Shakun, J.D., Singer, B.S., Mickelson, D.M., Refsnider, K.A., Caffee, M.W., 2006. Latest Pleistocene advance of alpine glaciers in the southwestern Uinta Mountains, Utah, USA. Evidence for the influence of local moisture sources. Geology 34, 841–844.
Munroe, J.S., Mickelson, D.M., 2002. Last Glacial Maximum equilibrium-line altitudes and paleoclimate, northern Uinta Mountains, Utah, U.S.A. Journal of Glaciology 48, 257–266.
Muzikar, P., Elmore, D., Granger, D.E., 2003. Accelerator mass spectrometry in geologic research. Geological Society of America Bulletin 115, 643–654.
O'Connor, J.E., 1993. Hydrology, hydraulics, and geomorphology of the Bonneville flood. Geological Society of America Special Issue, 273. 83 pp.
Oviatt, C.G., 1997. Lake Bonneville fluctuations and global climate change. Geology 25, 155–158.
Oviatt, C.G., Habiger, G.D., Hay, J., 1994. Variation in the composition of Lake Bonneville marl: a potential key to lake-level fluctuations and paleoclimate. Journal of Paleolimnology 11, 19–30.
Oviatt, C.G., Nash, W.P., 1989. Late Pleistocene basaltic ash and volcanic eruptions in the Bonneville basin, Utah. Geological Society of America Bulletin 101, 292–303.
Personius, S.F., and Scott, W.E., 1992. Surficial geologic map of the Sale Lake City segment and parts of adjacent segments of the Wasatch Fault Zone, Davis, Salt Lake, and Utah Counties, Utah: U.S. Geological Survey Miscellaneous Investigations Series Map I-2106, scale 1:50,000.
Porter, S.C., Pierce, K.L., Hamilton, T.D., 1983. Late Wisconsin mountain glaciation in the western United States. Late-Quaternary environments in the western United States. : In: Porter, S.C. (Ed.), The late Pleistocene, Volume 1. University of Minnesota Press, Minneapolis, MN, pp. 71–111.
Putkonen, J., Swanson, T., 2003. Accuracy of cosmogenic ages for moraines. Quaternary Research 59, 255–261.
Refsnider, K.A., Laabs, B.J.C., Plummer, M.A., Mickelson, D.M., Singer, B.S., Caffee, M.W., 2008. Last Glacial Maximum climate inferences from cosmogenic dating and glacier modeling of the western Uinta ice field, Uinta Mountains, Utah. Quaternary Research 69, 130–144.
Reimer, P.J., Baillie, M.G.L., Bard, E., Bayliss, A., Beck, J.W., Blackwell, P.G., Bronk Ramsey, C., Buck, C.E., Burr, G.S., Edwards, R.L., Friedrich, M., Grootes, P.M., Guilderson, T.P., Hajdas, I., Heaton, T.J., Hogg, A.G., Hughen, K.A., Kaiser, K.F., Kromer, B., McCormac, F.G., Manning, S.W., Reimer, R.W., Richards, D.A., Southon, J.R., Talamo, S., Turney, C.S.M., van der Plicht, J., Weyhenmeyer, C.E., 2009. IntCal09 and Marine09 radiocarbon age calibration curves, 0–50,000 years cal BP. Radiocarbon 51, 1111–1150.
Richmond, G., 1964. Glaciation of Little Cottonwood and Bells Canyons, Wasatch Mountains, Utah. U.S. Geological Survey Professional Paper, 454-D, pp. D1–D41.
Rosenbaum, J.G., Heil Jr., C.W., 2009. The glacial/deglacial history of sedimentation in Bear Lake, Utah and Idaho. Paleoenvironments of Bear Lake, Utah and Idaho, and its catchment: In: Rosenbaum, J.G., Kaufman, D.S. (Eds.), Boulder, Colorado, Geological Society of America Special Paper, 450, pp. 247–262.
Schaefer, J.M., Denton, G.H., Barrell, D.J.A., Ivy-Ochs, S., Kubik, P.W., Andersen, B.G., Phillips, F.M., Lowell, T.V., Schluechter, C., 2006. Near-synchronous interhemispheric termination of the Last Glacial Maximum in mid-latitudes. Science 312, 1510–1513.
Scott, W.E., 1988. Temporal relations of lacustrine and glacial events at Little Cottonwood and Bells canyons, Utah. In the footsteps of G.K. Gilbert; Lake Bonneville and neotectonics of the eastern Basin and Range Province; guidebook for field trip twelve: In: Machette, M.N. (Ed.), Salt Lake City, Utah, Utah Geological Survey Miscellaneous Publication, 88–1, pp. 78–81.
Scott, W.E., Shroba, R.R., 1985. Surficial geologic map of an area along the Wasatch Fault Zone in the Salt Lake Valley, Utah. U.S. Geological Survey Open File Report, 85–448. 19 pp.
Scott, W.E., McCoy, W.D., Shroba, R.R., Rubin, M., 1983. Reinterpretation of the exposed record of the last two cycles of Lake Bonneville, western United States. Quaternary Research 20, 261–285.
Stuiver, M., Grootes, P.M., 2000. GISP2 oxygen isotope ratios. Quaternary Research 53, 277–284.
Stone, J.O., 2000. Air pressure and cosmogenic isotope production. Journal of Geophysical Research, B, Solid Earth and Planets 105, 23,753–23,759.
Thackray, G.D., 2008. Varied climatic and topographic influences on Late Plesticene mountain glaciation in the western United States. Journal of Quaternary Science 23, 671–681.
Thackray, G.D., Lundeen, K.A., Borgert, J.A., 2004. Latest Pleistocene alpine glacier advances in the Sawtooth Mountains, Idaho, USA: reflections of midlatitude moisture transport at the close of the last glaciation. Geology 32, 225–228.
Torsnes, I., Rye, N., Nesje, A., 1993. Modern and Little Ice Age equilibrium-line altitudes on outlet valley glaciers from Jostedalsbreen, western Norway; an evaluation of different approaches to their calculation. Arctic and Alpine Research 25 (2), 106–116.
Ward, D.J., Anderson, R.S., Guido, Z.S., Briner, J.P., 2009. Numerical modeling of cosmogenic deglaciation records, Front Range and San Juan Mountains, Colorado. Journal of Geophysical Research 114, F01026.